Thermochimica Acta, 109 (1986) 11–28
Elsevier Science Publishers B.V., Amsterdam – Printed in The Netherlands

PROGRESS IN MODELING HEAT CAPACITY VERSUS TEMPERATURE MORPHOLOGY *

EDGAR F. WESTRUM, Jr. and NORIKAZU KOMADA **
Department of Chemistry, University of Michigan, Ann Arbor, MI 48109 (U.S.A.)
(Received 23 June 1986)

ABSTRACT

After discussion of other models for representing heat capacities, the volumetric model used in resolution of lanthanide Schottky contributions over the cryogenic range and a more recent single-parameter formula to represent the lattice heat capacity, to resolve excess heat capacity contributions, to extrapolate lattice heat capacity beyond the measured temperature regions, and to predict thermodynamic properties of a compound in a series of known isostructural compounds is described. It is based on a new phonon distribution function improved over the Debye model by distinguishing between transverse and longitudinal modes, differences in the masses of the constituent atoms, the actual shape of the first Brillouin zone, the discreteness of the crystal structure, etc. Several other parameters included in the formula are uniquely determined from chemical, crystallographic, and elastic data. The single characteristic temperature (θ), is retained in the formula as a parameter to be determined by fitting the calorimetric data. The success of the model was checked by plotting the apparent characteristic temperature against temperature for experimental heat-capacity data of compounds with purely lattice heat capacities.

INTRODUCTION

Modeling the heat capacity morphology is a matter of relating the thermophysical properties of condensed phases to atomic structures and vibrations. It is a task which even the experimentalist cannot avoid since the excess heat capacity related to a transition or to a Schottky function needs to be resolved from—except at very low temperatures—the typically greater lattice contribution.

* Based in part on project support from the Thermodynamics and Structural Program of the Division of Chemistry, National Science Foundation.
Dedicated to Professor Syûzô Seki in honor of his contribution to Calorimetry and Thermal Analysis.
** Present address: Mitsubishi Metals Incorporated, Nuclear Energy Department, Mitsubishi Metal Corporation, 1-6-1 Ohtemachi, Ohtemachi Building, 2nd Floor, Tokyo 100, Japan.

0040-6031/86/$03.50

The rather formidable problem of enumerating and quantifying the crystalline vibrational modes must be approached in order to account for the absolute values of the heat capacity and their derived thermophysical properties, especially the entropy. Having achieved this goal for certain substances greatly facilitates not only the interpolation of the lattice heat capacities across broad regions where the total measured heat capacity is somewhat greater, but encourages the prospect of estimating, or predicting, the heat capacities of related substances. Whether that relationship needs to involve isostructural crystals, crystals of the same coordination numbers, or even looser similarly may depend on the quality of the resolution achieved in the model. The problem is nearly a century old but there is still both need and hope for an enhancement of the results.

A dramatic step was induced in 1907 by Einstein's quantization of particle energy as a harmonic oscillator with three degrees of freedom and a unique vibration frequency corresponding to a characteristic temperature, θ_E [1]. Substantial differences between measured heat capacities and those predicted by the Einstein model led Nernst and Lindemann [2] to combine several (different) Einstein θ_E values in 1911 to achieve a better fit. (Much later (1955) Blackman [3] provided a basis for this approach.) However, the failings of the Einstein model triggered important development by Debye [4] in 1912 on a continuum model and, even more exciting, the independent analysis of Born and Von Kármán [5,6] on the lattice vibrational spectrum. Many others contributed to the solid-state vibrational theory, but inasmuch as we recognize a limited goal the full details of lattice dynamics are rather more than we can afford to cope with, particularly in the characteristic absence of thermal expansion values on crystals of interest.

OTHER MODELS

The gap between the simple Einstein [1] or Debye [4] models and the more rigorous Born–Von Kármán [5,6] treatment for the estimation of lattice heat capacity is large. Yet the estimation of lattice heat capacity is important in resolving excess heat capacities, in extrapolating heat-capacity curves beyond the temperature region measured, and in predicting the heat capacity of related compounds. The Debye model is still often used for these purposes because lattice heat capacity is fully described by essentially a single variable, the Debye characteristic temperature, which can be treated as a parameter to be determined by fitting the model to the heat-capacity curve or by invoking simple relationships with elastic constants, compressibility, or melting temperature. But the model generally provides an accurate estimate only for the extremely low-temperature region (typically below 1/50 of the Debye characteristic temperature) or for isotropic monatomic crystalline compounds.

On the other hand, the Born–Von Kármán formalism facilitates evaluation of an accurate density of vibrational modes as a function of frequency and the estimation of a more accurate lattice heat capacity. For the simplest case, the set of interatomic force constants required is obtained from inelastic neutron diffraction data, infrared spectra, Raman spectra, Brillouin and X-ray scattering data, and/or elastic and dielectric constants by the least-squares method, etc. The number of force constants in such procedures is, however, so large that many phonon models (e.g., ion shell, extended shell, overlap shell, deformation dipole, deformable shell, breathing shell, double shell, quadrupole shell, bond charge, valence force field, valence overlap shell model, three-body force shell model, etc.) have been used to reduce the number of parameters as well as to interpret phonon spectra. Since even these phonon models requires roughly ten parameters to represent the phonon distribution function for a simple compound and require additional data from sophisticated, slow neutron scattering experiments, etc., they are quite impractical for the routine analyses of heat-capacity data.

Many attempts already have been made to attain a reasonably simple and accurate model of phonon distribution for practical use. One of the most popular and convenient methods is to express lattice heat capacity as a combination of the Debye and Einstein functions. That is, two transverse acoustical modes (sometimes degenerate) and one longitudinal acoustical mode are approximated by a parabolic distribution which leads to a Debye function. Peaks in the distribution function for optical modes, most of which are also observed as peaks in infrared or Raman spectra, are represented by the Dirac δ-function which leads to an Einstein function.

The much more recent Kieffer model [7,8] has been particularly useful in mineralogy. Kieffer's theoretical and experimental correlation of the lattice vibrations of minerals takes into account the many factors involved and discusses particularly the analysis of the vibrational contribution. Kieffer divided the distribution function into three frequency groups. One comprises the acoustical modes. Their phonon distribution is derived from the application of the sinusoidal dispersion relation for a one-dimensional lattice to the three-dimensional vibrations. Three cut-off frequencies are obtained from the acoustical data. (Such a distribution was derived first by Barber and Martin [9].) The second group is the densely packed optical modes which are intuitively approximated by a constant phonon density. The low-end and high-end frequencies for this portion are obtained from infrared or Raman spectra. The optical modes of the frequencies which are outside of the second group form the third group. These modes, which usually belong to internal branches, are approximated by the Dirac δ-function. Though these semi-empirical approaches are very useful, especially for prediction of the lattice heat capacity from elastic and spectroscopic data, it is very difficult to derive a representative characteristic temperature and, therefore, useful relationships like the Lindemann equation or the Grüneisen

relation are not applicable unless each vibrational mode is considered independently [7]. Another problem with such methods is the impracticality of fitting them to the experimental heat-capacity curve because of the many parameters involved. Therefore, the application of these methods to the analysis of calorimetric data is confined to the comparison between predicted and experimental heat capacities when elastic and spectroscopic data are available.

Attempts to get an experimental estimate of C_{latt} in compound X by measuring the heat capacity of an isostructural diamagnetic compound ID are frequent. Here, the corresponding states assumption:

$$C_{\text{latt}}(\text{X})T = C_{\text{latt}}(\text{ID})/\kappa T$$

in which κ is experimentally deduced, is often employed.

Alternatively, the Debye θ_{D} approximation may be expressed in terms of the mass μ of the molecules:

$$\theta_{\text{D}}(\text{X})/\theta_{\text{D}}(\text{ID}) = \{\mu(\text{ID})/\mu(\text{X})\}^{1/2}$$

The more refined Lindemann relation using melting temperatures, T_{f}, and molar volumes V_{m}, is also used:

$$\theta_{\text{D}}^2 = \kappa' T_{\text{f}}/\mu V_{\text{m}}^{2/3}$$

Corresponding-states approaches are often used; but for more than half a century the Latimer scheme [10,11] has been a favorite way of taking into account the differences between compounds in iso-anionic series. This time-honored scheme, devised primarily for entropy estimates, is not without its flaws, despite the several times it was adjusted by Latimer himself.

THE VOLUMETRIC SCHEME FOR HEAT CAPACITIES

This scheme was developed at Ann Arbor by Westrum and others during extensive investigations of the Schottky contribution [5]. It involves linear interpolation on the basis of the molar volumes of the compounds in question. In particular, the formula by which the lattice heat capacity of praseodymium trihydroxide, for example, may be calculated as:

$$C_p\{\text{Pr(OH)}_3, \text{ lattice}\} = xC_p\{\text{La(OH)}_3\} + (1-x)C_p\{\text{Gd(OH)}_3\}$$

and in which x is the fractional molar volume increment, i.e.

$$x = [V_{\text{m}}\{\text{Pr(OH)}_3\} - V_{\text{m}}\{\text{La(OH)}_3\}]/[V_{\text{m}}\{\text{La(OH)}_3\}]$$

Here the lanthanum and the gadolinium compounds represent diamagnetic compounds isostructural with the praseodymium compound with $^1S_0$ ground states, and hence no Schottky contributions. It should be noted that utilization of other than linear interpolations would have involved differences in

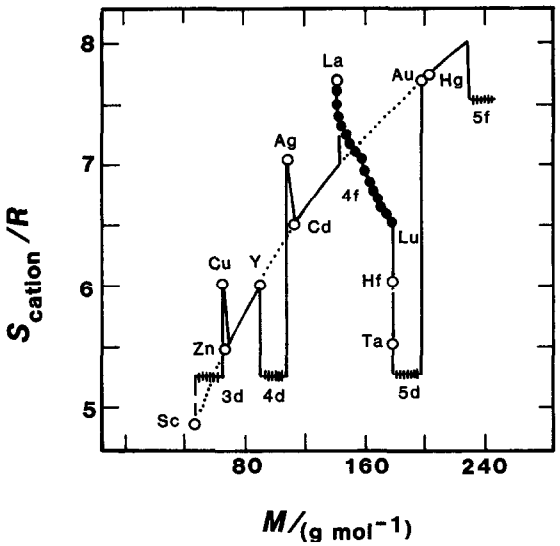

Fig. 1. Comparison of Grønvold and Westrum's scheme [15] against the background of the Latimer scheme (O · · · · · O). The Latimer-scheme contributions; (●), experimental values for the lanthanide cations [10,11]; (———) experimental values for the transition-elemental cations.

only second-order effects. The importance of volume was appreciated [13,14] on recognition of the fact that for the lanthanide chalcogenides the lattice contribution decreased with increasing atomic number and was, therefore, diametrically opposed to the trend in the Latimer scheme based on mass. The Grønvold/Westrum scheme [15] plus recognition of the lanthanide contraction provided the clue (Fig. 1). Other authors [16,17] have been engaged in a polemic as to the relevance of volume against mass in providing interpolation schemes for lattice contributions (cf. ref. 18).

An excellent test for the validity of a lattice-contribution scheme is in the calculation of the calorimetric Schottky contribution and the comparison of this excess heat capacity with that calculated from spectroscopic quantities on the samples themselves. This comparison can be made only when one utilizes the Stark levels of the concentrated compounds. Measurements made on doped lanthanide halides, for example, need to be extrapolated by some technique (discussed elsewhere [12]) or by calculations based on crystal-field parameters.

Several tests of the scheme on lanthanide trihydroxides and trichlorides

Since resolution of Schottky contributions from the generally much larger vibrational (lattice) heat capacities of lanthanide compounds has been limited by the uncertainty in the magnitude of the lattice contribution, such

subtle effects as dependence of the Stark levels on temperature and host lattice have been heretofore undetected calorimetrically.

Since the lanthanide trihydroxides are an iso-anionic series having relatively small lattice contributions and their lower-lying Stark levels have been spectroscopically deduced for many of the concentrated compounds, this series is the most nearly ideal system we have yet studied in an attempt to resolve Schottky contributions in the 5–350 K range. Three examples illustrate the success of the scheme described on $Ln(OH)_3$ systems.

$Eu(OH)_3$. The Schottky contribution to the heat capacity of the Eu(III) analog [19] is unique in that it arises entirely from thermal populations of excited [SL] J-manifolds. This invariably results in the lowest-excited Stark levels being much higher in energy for the Eu(III) analog than for any other series member. The calculated Schottky heat capacity is consequently relatively insensitive to small shifts in the Stark energies and, therefore, is expected to be the most accurate approximation to the true Schottky heat capacity within any lanthanide series.

The energy levels of concentrated $Eu(OH)_3$ were determined by Cone and Faulhaber [20] from absorption and fluorescence spectra at 4.2 and 7.7 K. Stark levels arising from the $^7F_0$, $^7F_1$, $^7F_2$, and $^7F_3$ manifolds all contribute to the Schottky heat capacity below 350 K. The derived calorimetric Schottky contribution shown in Fig. 2 is seen to be in excellent accord with that calculated from the spectroscopic quantities [21].

$Pr(OH)_3$. The crystal-field splitting of the $^3H_4$ manifold of $Pr(OH)_3$ has been determined from the absorption spectra of mulls at 95 K [22]. The observed spectra were not as highly resolved as those one might obtain from measurements on single crystals. This lack of resolution is reflected in a ± 3 cm^{-1} uncertainty in the Stark wavenumbers. As seen in Fig. 2 the calorimetric and spectroscopic Schottky curves are in very good agreement between 15 and 230 K. Below 25 K a cooperative magnetic contribution of unknown magnitude plus the uncertainty in the energy of the lowest-excited Stark level preclude any attempt to determine the Schottky contribution accurately in this temperature region.

$Tb(OH)_3$. The energy levels of the lowest four manifolds of concentrated $Tb(OH)_3$ and Tb^{3+}-doped $Y(OH)_3$ were determined by Scott et al. [23]. The observed Schottky anomaly below 350 K is due almost entirely to population of the $^7F_6$ manifold. The availability of spectroscopically determined energy levels for both the $Tb(OH)_3$ and $Y(OH)_3$ host lattices provides an opportunity to observe directly the sensitivity of the new lattice-contribution approximation technique in differentiating between such systems. Heretofore the general assumption has been that any calorimetrically derived Schottky contribution is too crude to detect the effect of any differences in the Stark level energies of such systems.

As seen in Fig. 2 the calorimetric and calculated $Tb(OH)_3$ Schottky curves are in excellent agreement below 160 K, while at higher temperatures

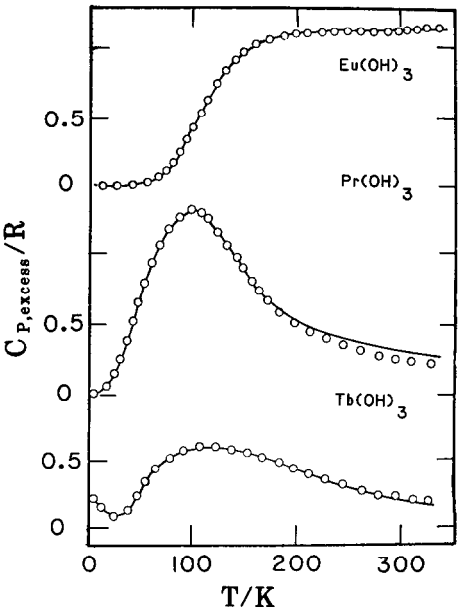

Fig. 2. Schottky heat-capacities for several lanthanide trihydroxides. (———) Spectroscopic Schottky contributions; (O) calorimetric Schottky contributions resolved by the volumetric method.

the calorimetric curve trends below that deduced from the spectral quantities [24].

Iso-anionic lanthanide series and general isostructural series. Thus the trend in lattice heat capacities of iso-anionic series of lanthanide compounds may be rationalized in terms of two contributing factors: molar mass and molar volume. At low temperatures, the lattice contribution is due primarily to thermal activation of acoustic lattice modes and molar mass is the dominant factor. At higher temperatures increasing thermal activation of optical lattice modes, which are strongly affected by the lanthanide contraction, results in lattice heat capacities which are related predominantly to the trend in molar volume. For the light lanthanide trihydroxides the molar-mass variation is dominated by the molar-volume effect at least above 50 K. Only for much lighter $Y(OH)_3$ is the mass effect clearly visible and then only below 100 K.

Hence, in emphasizing the importance of volume, we do not mean to slight mass; especially not at lower temperatures. Results for $U(OH)_3$, which is isostructural with the $Ln(OH)_3$'s should help to clarify and to test the role of mass. Although we have demonstrated the great utility of the volumetric scheme as an interpolation device for $C_p(T)$ or $S^0(298\ K)$ for a system of isostructural compounds, what about the broader implications? How generally does it supplant the Latimer rule even when "augmented" to provide magnetic contributions, etc.?

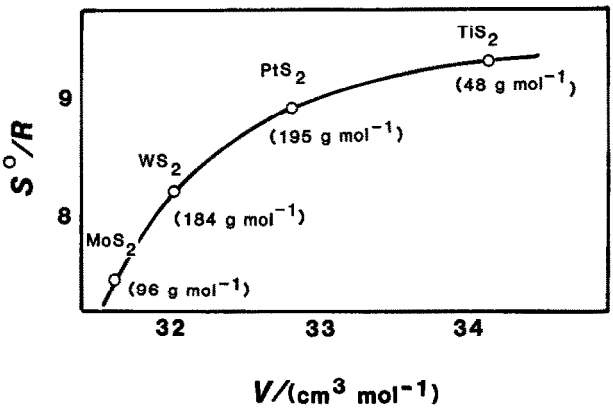

Fig. 3. Correlation of entropies and molar volumes. The values in parentheses are molar masses of the cations.

We have examined isostructural series on which sufficient results exist to make a judgment. Many interesting trends are observed. For example, as seen in Fig. 3, extrapolation by the Latimer scheme from the entropies (298 K) of MoS_2, WS_2, PtS_2 to that of TiS_2 would lead to a Latimer-scheme value of $S^0/R = 7$; on the other hand the volumetric approach would lead to $S^0/R = 9.5$. Experiment ($S^0/R = 9.4$) confirms the latter. In other instances the general trend of cation mass with molar volume in iso-anionic series often tends to make choice between the two systems difficult inasmuch as molar mass and molar volume usually go hand-in-hand. Identification of key compounds on which to test the scheme and to develop more reliable correlations is underway. The broadening of these schemes has gone more slowly than anticipated since the non-conformity often seems to signal an interesting excess contribution.

In total the lanthanide sesquioxides [25–27] have been studied at Ann Arbor, the lanthanide trichlorides [28,29], the lanthanide trihydroxides [24,30–32], the lanthanide hexaborides [33], and work on the lanthanide sesquisulfides is also nearly complete [34].

In the above discussion, frequent reference is made to Schottky contributions [35], interesting in their own right, but used here initially and primarily as a means of testing the success of the evaluation of the lattice contribution.

THE SINGLE PARAMETER PHONON DISTRIBUTION MODEL

We developed a new model for the phonon distribution [36] characterized by a single characteristic temperature as a fitting-parameter for the analysis and/or prediction of the thermodynamic properties. Although the equation derived from the model to calculate the lattice heat capacity at constant

volume is somewhat lengthy, it is simple enough to manage even on a microcomputer. Three computer programs written in FORTRAN IV were prepared to evaluate apparent characteristic temperatures from given heat-capacity data, to predict lattice heat capacities from the given characteristic temperatures, and to compare the predicted and given (possible experimental) heat capacities. These programs ensure the convenient analysis of heat-capacity data. The model has already proven its utility in treating experimental data on eight compositions of matter ($Mn_{0.63}Cr_{0.37}As$, deerite, grunerite, and some scapolites) which will be published soon. It is rapidly being enhanced and adapted to related problems.

Treatment of transverse and longitudinal acoustical branches. Irrespective of chemical or crystallographic structure, any solid substance has two transverse acoustical and one longitudinal acoustical modes. In the model calculation, it is assumed that the two transverse acoustical modes are degenerate and the dispersion relation for the longitudinal acoustical mode is similar to the transverse modes. The first assumption holds only for the phonons which propagate in highly symmetrical directions such as [100] and [111] in the NaCl-type crystals and is not true in general. Since the dispersion relations for the two transverse acoustical modes are, however, quite similar in comparison to those for the longitudinal acoustical mode or the optical modes and have very similar peak frequencies, the assumption is probably not over-bold. The propriety of the second approximation may be judged from the typical example of dispersion relations [36].

Treatment of optical branches. It is not as easy to formulate the dispersion relations or the distribution function for the optical branches as for the acoustical branches as discussed above. Only the number of modes pertaining to the optical branches is easily obtained. That is, if the number of atoms in a formula unit or a molecule and that of formula units or molecules in a primitive cell are n and Z, there are $(3nZ - 3)$ optical branches per primitive cell or $(3n - 3/Z)$ per formula unit or molecule because the total number of degrees of freedom is $3nZ$ and three modes out of $3nZ$ modes are accommodated by the acoustical branches. The $(3nZ - 3)$ optical branches may be divided into $(2nZ - 2)$ transverse modes and $(nZ - 1)$ longitudinal model since any elastic wave which propagates in a three-dimensional medium is generally composed of two independent transverse modes and one longitudinal mode and thus phonon modes also may be automatically divided into two with the same ratio.

The frequency range

The wavelength corresponding to the maximum frequency for the acoustical branch at the edge of the first Brillouin zone is twice the size of the primitive cell. On the other hand, simple considerations on the properties of waves show that the wavelength cannot be smaller than twice the smallest

interatomic distance or the smallest spacing between the adjacent atomic planes which vibrate collectively. The maximum frequency for the acoustical branch is $(2k/\overline{M})^{-1/2}$ on the average mass approximation and the frequency is inversely proportional to the wavelength if the velocity is constant. If these facts are boldly related despite the standing wave at the zone boundary, the maximum frequency for the optical modes can be estimated on the average mass approximation:

$$\omega_m^O = (D/d)\,\omega_m^A$$

where D is the representative size of the primitive cell, d is the smallest interatomic distance or the smallest spacing of the atomic planes, and $\omega_m^A = (2k/\overline{M})^{1/2}$ is the maximum frequency for the acoustical mode on the average mass approximation. D may be the cube-root of the volume of the primitive cell (V), and d may be the smallest spacing of the atomic planes like that of the [111] planes in the NaCl structure. Since even in a simple structure the planes are generally composed of different kinds of atoms which interact with different force constants, the collective motion as a single plane is not expected. Therefore, d is for most cases the smallest interatomic distance. The smallest sum of the ionic radii of the possible pairs in the structure may be a good approximation for d if the crystallographic data are not available.

The lowest frequency for the optical mode coincides with ω_m on the average mass approximation. As the transverse and longitudinal acoustical modes are distributed in the different frequency ranges, the corresponding $(2nZ-2)$ transverse and $(nZ-1)$ longitudinal optical modes wil be distributed from $\omega_{m,T}^A$ to $(V^{1/3}/d)\omega_{m,T}^A$ and from $\omega_{m,L}^A$ $(V^{1/3}/d)\omega_{m,L}^A$ as the first approximation. The ratio of the longitudinal optical frequency to the transverse optical frequency ω_L^O/ω_T^O at low wave vector K can be related to the dielectric constants by the Lyddane–Sachs–Teller relation:

$$\left(\omega_L^O/\omega_T^O\right)^2 = \epsilon(0)/\epsilon(\infty)$$

where $\epsilon(0)$ is the static dielectric constant and $\epsilon(\infty)$ is the high-frequency limit of the dielectric function, defined to include the core electron contribution.

The frequency range in the first approximation is, however, too narrow since the masses of the atoms and the interatomic force constants are not identical in general and they both affect the vibration so that the frequency range becomes wider than that obtained from the average mass and the average force constant model. The heavier atoms with mass of M_h will lower the lowest frequency by the factor $(\overline{M}/M_h)^{1/2}$ and the lighter atoms with mass of M_l will raise the highest frequency by the factor $(\overline{M}/M_l)^{1/2}$ if the force constants are the same. The factor is deduced from the general mass dependency of the frequency. The phonon densities of the added frequency regions will be dominated by the numbers of the heavier and lighter atoms

in the primitive cell. It is, however, not easy to find the deviation of force constants from the average force constant in comparison to the mass factor if no additional data are provided except for the basic information such as the chemical and crystallographic structures. Therefore, the effects of different force constants are neglected in the model except for the special case of internal branches which will be discussed later.

The form of the distribution function. Were constant group velocity to be assumed as a first approximation, the phonon density would be a simple parabolic function of frequency like the Debye model under the continuum approximation. The major factor which changes the distribution function is the discreteness of the atomic arrangement in the real crystals because the wavelength is comparable to the interatomic distances. The discreteness is incorporated with brevity into the distribution function so that the phonon mode can exist by resonance only when one-half of its wavelength is approximately equal to a certain interatomic distance. The probability of this resonance is very roughly a parabolic function of wavelength since the number of atoms in the spherical shell is roughly proportional to the area of the sphere if its thickness is kept at an infinitesimally small constant value and the area is a parabolic function of radius. The probability of finding an interatomic distance close to a given value is directly proportional to the number of atoms which are located at the same distance from an arbitrarily chosen atom. Therefore, the parabolic distribution function based on the continuum approximation will be reduced by the factor which is inversely proportional to the square of frequency. The product is a simple constant phonon density independent of frequency. This result agrees with Kieffer's intuitive choice as described briefly in the Introduction. The low-frequency protrusion from $(2k/\overline{M})^{1/2}$ to $(2k/M_h)^{1/2}$ has a similar constant distribution function, and the high-frequency tail from $(2k/\overline{M})^{1/2}(V^{1/3}/d)$ to $(2k/M_l)^{1/2}(V^{1/3}/d)$ has a function of the form:

$$g(\omega) \propto 1 - \left(\omega/\omega_m^O\right)^2$$

where $\omega_m^O = (2k/M_l)^{1/2}(V_{1/3}/d)$. The reason for the choice of this equation is that the correction factor for discreteness shifts from ω^{-2} to $(\omega^{-2} - \omega_m^{O-2})$ at the high-frequency end because the phonon density is zero above ω_m^O. Many observed distribution functions curve toward zero in a manner similar to that of this equation. The magnitude of the low-frequency protrusion is determined so that the heavier atoms contribute to the phonon density homogeneously from $(2k/M_h)^{1/2}$ to $(2k/\overline{M})^{1/2}(V^{1/3}/d)$. The magnitude of the phonon density in the region from $(2k/\overline{M})^{1/2}$ to $(2k/M_l)^{1/2}(V^{1/3}/d)$ is determined so that the remaining degrees of freedom are exhausted. The distribution function for the high-frequency tail is determined from the condition for the continuity of the distribution function for the main portion at $\omega = (2k/M)^{1/2}(V^{1/3}/d)$. The last condition is quite arbitrary although it affects the heat-capacity curve only slightly.

Treatment of internal branches. Some molecular groups like OH^-, NH_4^+, SO_4^{2-}, and CO_3^{2-} form internal branches. The molecular group with s atoms has $(3s-6)$ internal branches if it is non-linear and $(3s-5)$ internal branches if it is linear. The frequency of each branch is little affected by the surroundings. Since their frequencies in the free ion state are well known for most cases and the frequencies in the crystal are not so different from those in the free ion state, the Dirac δ-function at the known frequency in the free ion state can represent the phonon density for the internal branch without serious error. Of course, better fit is expected if the frequency in the crystal is available. The molecular group has five or six degrees of freedom after the internal vibrations are subtracted as the internal branches. The molecular group may be regarded as a single particle with three normal vibrational modes for three independent directions (x, y, z) and three independent rocking motions (roll, pitch, and yaw) if it is non-linear. Or, alternatively, the molecular group may be regarded as two normal particles each of which has three degrees of freedom. (The linear molecular group has two independent rocking modes instead of three, and three normal vibrational modes.) Therefore, it may be assumed that the molecular group behaves as if there were 5/3 normal particles provided the internal branches are treated separately.

Certain vibrational modes may have exceptionally low or high frequencies because of extremely small or large force constants and/or because of the participation of exceptionally heavy or light atoms. For instance, the Si–O stretching mode, which has a frequency of ca. 1000 cm^{-1}, is isolated from the other modes in the phonon distributions of many silicates. These types of vibrational modes are more appropriately represented by Dirac δ-functions rather than by the constant phonon density though their frequencies may be more strongly affected by the circumstances than the "true" internal branches are. We recognized that isolated high-frequency modes appear upon the introduction of a few light atoms and that they can be properly approximated by the Dirac δ-function.

Formulation of the heat-capacity equation. The following characteristic temperature is used for a reference parameter in the formulation of the molar isometric heat capacity, $C_{v,m}(T)$ at the temperature T:

$$\theta = (h/2\pi k_B)(2k_T/M)^{1/2}$$

where h is the Planck constant, K_B is the Boltzmann constant, the subscript T of the force constant, k, denotes the transverse mode, and M is the arithmetic mean of atomic masses. This characteristic temperature corresponds to the maximum frequency for the doubly degenerate, transverse acoustical mode in the mean mass and the spherical Brillouin zone approximations and to about 90% of the maximum frequency for that mode in the Debye approximation.

The crystal with n atoms per formula unit or per molecule and with Z

formula units or molecules per primitive cell has a molar heat capacity at the infinitely high temperature in the Dulong–Petit limit, $3nR$, where R is the gas constant. If there are p internal branches in a primitive cell and the i-th internal branch is w_i-fold degenerates, the internal branches contribute

$$R\sum_{i=1}^{p} w_i/Z$$

to the heat capacity at their limit. The mean mass, M, should be calculated by:

$$\overline{M} = \sum_{i=1}^{n} M_i/\left(n - 1/3\sum_{i=1}^{n} w_i/Z\right)$$

Here M_i is the mass of the i-th atom in a formula unit or a molecule. The contributions of the transverse and longitudinal acoustical branches are $2R/Z$ and R/Z, and those of the transverse and longitudinal optical modes are

$$\left(2n - 2/Z - 2\sum_{i=1}^{n} w_i/3Z\right)R \text{ and } \left(n - 1/Z - \sum_{i=1}^{p} w_i/3Z\right)R$$

at their limits. Two-thirds of the internal branches are regarded as transverse and the rest as longitudinal modes. The general relationship between the distribution function, $g(\omega)$, and the isometric heat capacity, $C_v(T)$, is:

$$C_v(T) = \int_0^{\omega_{max}} \frac{\exp(\hbar\omega/k_B T)}{\{\exp(\hbar\omega/k_B T) - 1\}^2}\left(\frac{\hbar\omega}{k_B T}\right)^2 g(\omega)\, d\omega$$

where ω_{max} is the maximum frequency and $\hbar = h/2\pi$.

The molar lattice heat capacity at constant volume is the sum of the above five contributions:

$$C_{v,m}(T) = C_{v,m}^{TA}(T) + C_{v,m}^{LA}(T) = C_{v,m}^{TO}(T) + C_{v,m}^{LO}(T) + C_{v,m}^{T}(T)$$
$$= C_{v,m}(O, T) \qquad (1)$$

upon assumption of harmonic vibrations. The important feature of eqn. (1) is representation of the heat capacity as a function of the characteristic temperature, θ, for those compounds which do not have an internal branch. Equation (1) is a weighted sum of the terms which belong to one of the following two forms:

$$f(x) = \left[3/(Ax)^3\right]\int_0^{Ax} y^4 e^4/(e^y - 1)^2\, dy$$

$$g(x) = [3/Bx]\int_0^{Ax} y^2 e^2/(e^y - 1)^2\, dy$$

where A and B are constants and $x = \theta/T$.

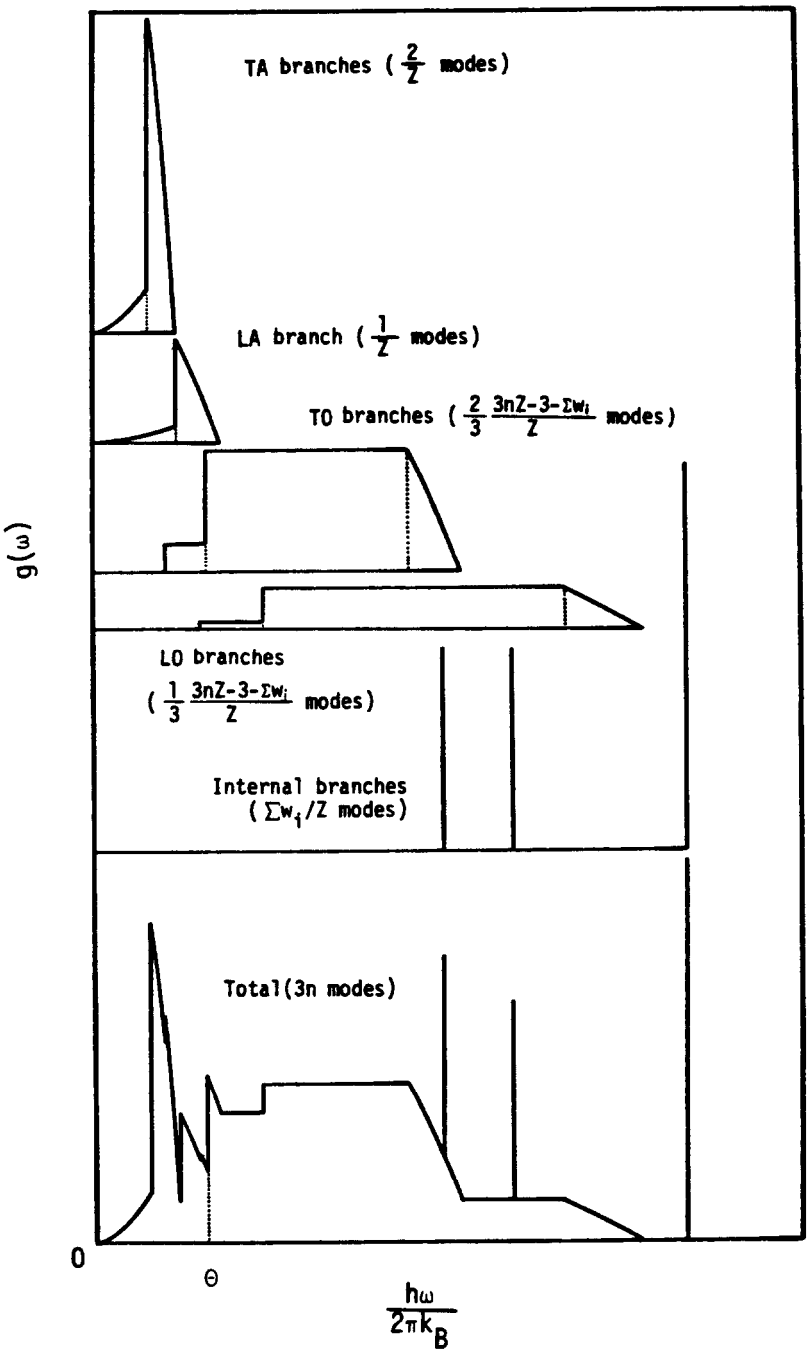

Fig. 4. Schematic distribution function for phonon distribution model.

The general morphology of the distribution function is shown in Fig. 4. Details of the evaluation of the particular models should be sought in the definitive paper [36].

Application of the model. One striking example of those cited is that of the scapolites [37]. Scapolite is a framework silicate mineral which can be regarded as a solid solution between two end-members: marialite, $Na_4Al_3Si_9O_{24}Cl$, and meionite, $Ca_4Al_6Si_6O_{24}CO_3$. The sub-ambient heat capacities of five scapolite members have been measured recently in our laboratory [37]. Our phonon distribution model was tested with those data since they do not have heat-capacity anomalies or electronic contributions below 350 K and they contain a significantly large number of atoms in the primitive cell.

The ratio ω_L/ω_T calculated for alkali halides on the basis of the simple Born model was used as that for scapolite since the related data to estimate ω_L/ω_T are not available. These were fit with parameters shown elsewhere [37] with an appropriate Brillouin zone (a rectangular parallelopiped), primitive-cell volume dependent on concentration and internal vibrations for carbonate and sulfate groups. Anharmonic effects were neglected because the heat capacities are less than 75% of the Dulong–Petit limit below 350 K.

The apparent characteristic temperatures thus calculated are shown in Fig. 5 and compared with the Debye characteristic temperatures also indicated in the same figure. The maximum characteristic temperature changes in the temperature region from 8 to 350 K average 15%, those for the Debye θ by 15%.

The improvement over the Debye model is clearly significant for the scapolite samples. The rise in the apparent θ at the low-temperature end for the Me_{55} sample is thought not to be due to a flaw of the model but to experimental problems.

Other applications of the theory are to the resolution of broad transitions in deerite [38], grunerite [38], and in $Mn_{0.63}Cr_{0.37}As$ [39]. Other applications including those to disilicate crystals and vitreous phases [40] and to the resolution of Schottky contributions in lanthanide sesquisulfides [41] are underway. Moreover, modifications of the theory itself are in progress.

Application to Grüneisen and Lindemann relations. The volume dependency of the Helmholtz free energy—an anharmonicity effect—is described by the volume dependency of θ; the equation of state for solids has the same form as that derived by Debye:

$$p = \delta E_0/\delta V = \Gamma(E_{\text{lattice}}/V)$$

where p is the pressure, E_0 is the internal energy at zero Kelvin (which is not a function of T), and Γ is the Grüneisen constant defined in terms of the characteristic temperature in our phonon distribution instead of by the Debye characteristic temperature. And, therefore, the Grüneisen relation, $\Gamma = \alpha V/\kappa C_v$ is compatible with the new model. Here, α is the volumetric

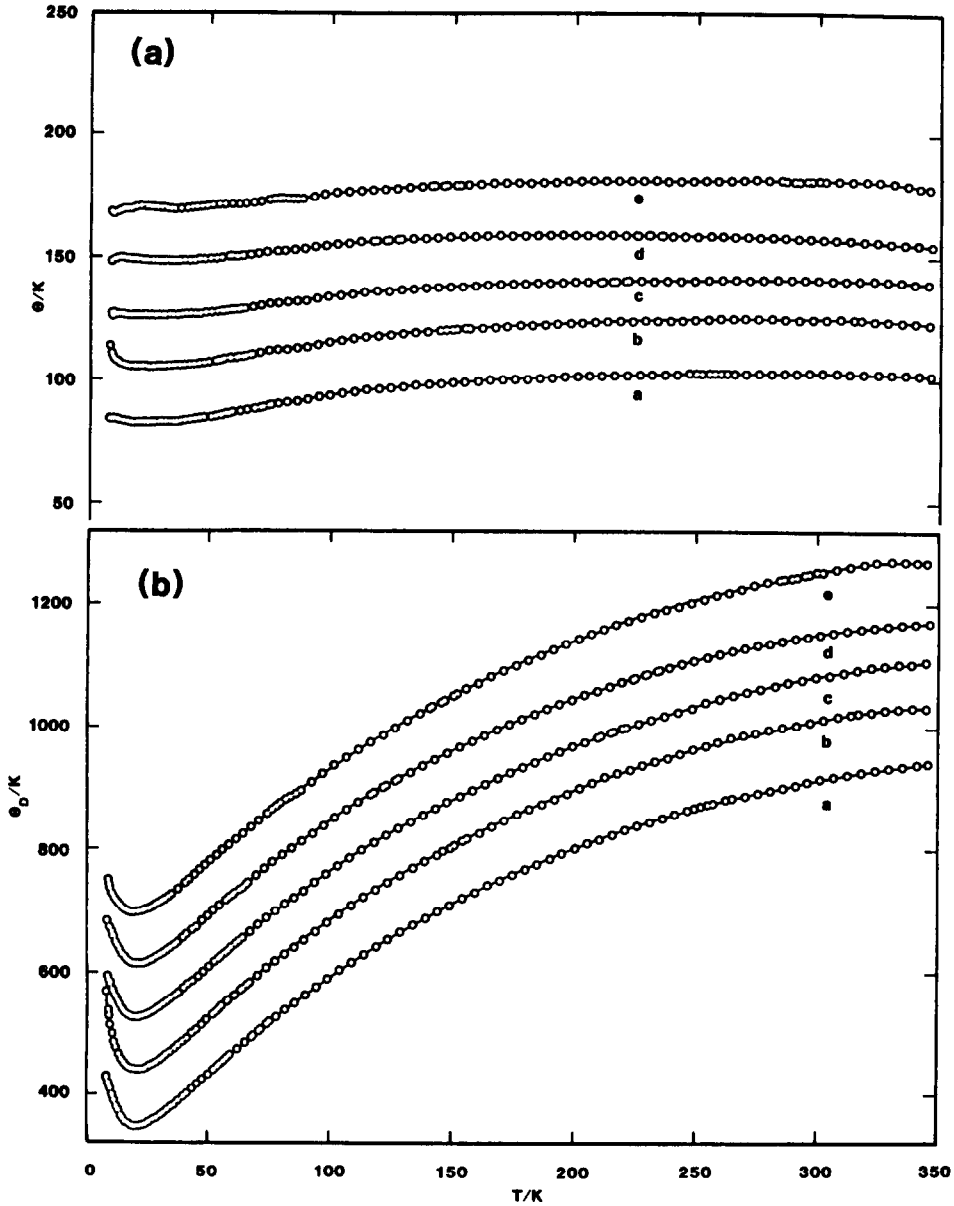

Fig. 5. (a) Temperature dependencies of the apparent characteristic temperatures for the five scapolite samples: (a) Me_{28}, (b) Me_{44}, (c) Me_{55}, (d) Me_{69}, (e) Me_{88}. The curves are displayed by 20 K increments to avoid overlap. The scale accords with values for Me_{28}. (b) Similar plot for Debye characteristic temperatures except that the increment is 89 K. The scale accords with values for Me_{28}.

thermal expansion coefficient and κ is the isothermal compressibility.

The Lindemann relation, based on a simplified model of the melting process, is also anticipated from the similarity between the general form of

the heat-capacity functions of the Debye model and the new model. That is,

$$\theta \propto T_m^{1/2} \bar{M}^{1/2} V^{-1/3}$$

where θ is the weighted average of θ and $(\omega_L/\omega_T)\theta$, $\theta = [3/\{2(\omega_L/\omega_T)^3 - 1\}]^{1/3}$ and T_m is the melting temperature.

Another practical utilization of the characteristic temperature is for the calculation of the apparent characteristic temperature from a single set of $(C_{v,m}, T)$ data. The extrapolation or interpolation of the apparent θ–T curve, which is expected to be insensitive to the temperature, may provide an attractive method for interpolation of lattice $C_{v,m}$ for resolution of the excess heat capacity or extrapolation of lattice $C_{v,m}$ into an unmeasured temperature region.

Computer programs for application of the model. Three computer programs (suitable even for microcomputers) written in FORTRAN IV were prepared for the convenient application of the equation with complete instructions for the input data file prior to each program statement. They are listed elsewhere in their entirety [42].

REFERENCES

1 A. Einstein, Ann. Phys., 22 (1907) 180; 35 (1911) 679.
2 W. Nernst and F.A. Lindemann, Berl. Ber., (1911) 494.
3 M. Blackman, The specific heat of solids, in Handb. Phys., 7(1) (1942) 325.
4 P. Debye, Zur Theorie der spezifischen Warmen, Ann. Phys., 39(4) (1912), 789.
5 M. Born and T. von Kármán, Z. Phys., 13 (1912) 279.
6 M. Born and T. von Kármán, Z. Phys., 14 (1913) 65.
7 S.W. Kieffer, Rev. Geophys. Space Phys., 17 (1979) 1, 20, 35, 862; 20 (1982) 827.
8 S.W. Kieffer, in S.W. Kieffer and A. Navrotsky (Eds.), Microscopic to Macroscopic, Reviews in Mineralogy, Vol. 14, Mineralogical Society of America, Washington, DC, 1985.
9 S.W. Barber and B. Martin, J. Phys. Chem. Solids, 9 (1959) 198.
10 W.M. Latimer, J. Am. Chem. Soc., 43 (1921) 1186.
11 W.M. Latimer, J. Am. Chem. Soc., 73 (1951) 1480.
12 E.F. Westrum, Jr., J. Chem. Thermodyn., 15 (1983) 305.
13 E.F. Westrum, Jr., Usp. Khim., 48 (1979) 2194.
14 E.F. Westrum, Jr., Russ. Chem. Rev., 48 (1979) 1186.
15 F. Grønvold and E.F. Westrum, Jr., Inorg. Chem., 1 (1962) 36.
16 S.K. Saxena, Science, 193 (1976) 1241.
17 S. Cantor, Science, 198 (1977) 206.
18 E.F. Westrum, Jr., in F.R. Gould (Ed.), Lanthanide/Actinide Chemistry, Am. Chem. Soc., Washington, DC, 1967, p. 25.
19 E.F. Westrum, Jr., R.D. Chirico and J.B. Gruber, J. Chem. Thermodyn., 12 (1980) 717.
20 R.L. Cone and R. Faulhaber, J. Chem. Phys., 55 (1971) 5198.
21 R.D. Chirico and E.F. Westrum, Jr., J. Chem. Thermodyn., 12 (1980) 71.
22 Reference 23 together with unpublished spectra cited in Table 1 therein.
23 P.D. Scott, H.E. Meissner and H.M. Crosswhite, Phys. Lett. A, 28 (1969) 489.
24 R.D. Chirico and E.F. Westrum, Jr., J. Chem. Thermodyn., 13 (1981) 519.

25 B.H. Justice and E.F. Westrum, Jr., J. Phys. Chem., 67 (1963), 339, 345, 659.
26 B.H. Justice, E.F. Westrum, Jr., E. Chang and R. Radebaugh, J. Phys. Chem., 73 (1969) 333.
27 B.H. Justice and E.F. Westrum, Jr., J. Phys. Chem., 73 (1969) 1959.
28 J.A. Sommers and E.F. Westrum, Jr., J. Chem. Thermodyn., 8 (1976) 1115; 9 (1977) 1.
29 E.F. Westrum, Jr., R.D. Chirico and J.B. Gruber, J. Chem. Thermodyn., 12 (1980) 717.
30 R.D. Chirico, E.F. Westrum, Jr., J.B. Gruber and J. Warmkessel, J. Chem. Thermodyn., 11 (1979) 835.
31 R.D. Chirico and E.F. Westrum, Jr., J. Chem. Thermodyn., 12 (1980) 71, 13 (1981) 519.
32 R.D. Chirico, E.F. Westrum, Jr. and J. Boerio-Goates, J. Chem. Thermodyn., 13 (1981) 1087.
33 E.F. Westrum, Jr., H.L. Clever, J.T.S. Andrews and G. Feick, in L. Eyring (Ed.), Rare Earth Research, III, Gordon and Breach, New York, 1966, p. 597.
34 E.F. Westrum, Jr. et al., unpublished results.
35 W. Schottky, Phys. Z., 23 (1922) 448.
36 N. Komada and E.F. Westrum, Jr., in preparation.
37 N. Komada, D.P. Moecher, E.F. Westrum Jr. and B.J. Hemingway, J. Chem. Thermodyn., submitted.
38 N. Komada, E.F. Westrum, Jr. L. Anowitz, and B.J. Hemingway, J. Chem. Thermodyn., submitted.
39 N. Komada, E.F. Westrum, Jr., H. Fjellvag and A. Kjekshus, Magn. Magn. Mater., in press.
40 E.F. Westrum, Jr. and A.K. Labban, in preparation.
41 E.F. Westrum, Jr. and J. Gruber, in preparation.
42 NAPS Repository Document to accompany ref. 36 (cf. ref. 36).